The influence of joining technique on the deformation of laser welded T-joints

Wiesława Piekarska[1*], *Zbigniew* Saternus[1], *Milan* Sapieta[2], and *Peter* Kopas[2]

[1]Czestochowa University of Technology, Faculty of Mechanical Engineering and Computer Science, Czestochowa, Poland
[2]University of Žilina, Faculty of Mechanical Engineering, Žilina, Slovak Republic

Abstract. T-joints are often used in large-scale welded constructions. The use of a laser beam for welding allows to create joints using various techniques. Used welding method affects the shape and size of heat affected zone, deformation of welded elements and consequently the quality of the joint. This work concerns the numerical modeling of the size of heat affected zone and welding deformations in T-joint obtained with two different welding techniques: single-side fillet T-joint and butt welded T-joint, called I-core welded joint. Numerical simulations are carried out in the commercial Abaqus FEA software, supplemented by an additional numerical subroutines which enabled the analysis of thermomechanical phenomena occurring in welding process. Mathematical model of a moveable welding source and the description of heat source positioning relative to the edges of the connected elements are described in numerical subroutines. The material parameters of austenitic steel are taken into account. The size of deformations of welded joints are determined as well as the influence of two different joininig techniques of T-joint on the amount of generated welding deformations are analyzed and compared.

Keywords: Abaqus software, numerical modelling, laser welding, T-joint welded joint, welding deformations

1 Introduction

Laser technology is used in the manufacture of many types of welded joints. T-joint are commonly used in the industry. Modern welding equipment based on a laser beam introduced to the industry has greatly increased the ability to perform laser welded T-joints [1, 2]. The laser welding allows to produce T-joints using various welding techniques. Joints in the laser welding process are characterized by a small amount of heat introduced into the joint. This has a significant impact on its strength properties [2, 3]. The welding process due to the deep penetration of the laser beam into the material allows the use of very high welding speeds [3, 4].

* Corresponding author: piekarska@imipkm.pcz.pl

Reviewers: *Justín* Murín, *Konrad* Waluś

The classical fillet welds require the use of additional material. In the case of single-side welding of T-joint [3, 5] or I-core type [6, 7], the additional material is omitted. An important problem that arises in the absence of additional material is the need for a precise set-up of joined surfaces. The gap between the elements should be close to zero [3]. The high precision of welds obtained in the laser welding process allows to perform I-core joint type. During welding process usig this method, the laser beam penetrates through the outer surface of one of the sheets and merges it into the stiffening element [8].

Coupled thermomechanical phenomena have a direct impact on the quality of the resulting joint in the laser welding process [9-12]. Conducting experimental research is quite expensive, therefore in order to understand the welding phenomena, numerical research is increasingly performed. Numerical research requires the development of appropriate mathematical and numerical models to properly perform the conditions of the welding process [4, 5].

The paper presents numerical analysis of thermomechanical phenomena of the laser welding process of T-joint using various welding techniques. The first welding technique is single-side butt welding (Fig. 1a) while the second connection is the welding T-joint using the I-core type joint (Fig. 1b).

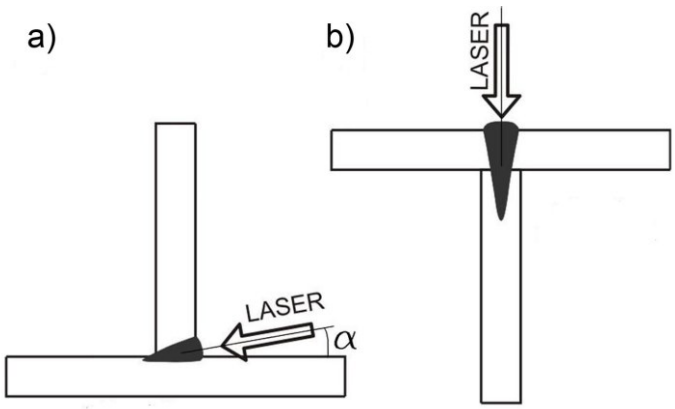

Fig. 1. Scheme of laser welded T-joint: a) single side butt welded joint, b) I-core T-joint

The three-dimensional numerical models is developed on the basis of dimensions and technological parameters presented in publication [3]. Numerical investigations are made in the Abaqus FEA software. The basic form of Abaqus program has been expanded by additional subroutines. In DFLUX subroutine the power distribution of the moving heat source and the slope relative to the connected elements is modeled. The material of joined sheets is stainless steel 304 (X5CrNi18-10). In the numerical model, thermomechanical properties variables with temperature 304 steel were taken into account [4, 11]. The calculations are performed for two different tee welding techniques using a laser beam. In both cases, the same process parameters were used (laser beam power and welding speed).

Temperature distribution in welded joints, shape of melting zone are determined. In the case of single-side welding, the obtained results were compared with the experience. On the basis of the conducted analysis of mechanical phenomena, the stress state in the weld and welding deformations in T-joints are numerically estimated.

2 Finite element model

The analysis of thermomechanical phenomena of laser welding process of T-joint is carried out in the Abaqus FEA program. The influence using two different welding techniques: the

butt one-sided welding and the connection of the I-core type is analyzed. For each case the appropriate three-dimensional discrete models is developed in the calculation program. The geometrical dimensions of welded sheets are: 30x100x3 mm and 30x100x1 mm, according to the diagram shown in Figures 2a and 2b. The adopted dimensions are based on studies included in the literature [3]. The technological parameters of the welding process are also taken from the literature [3]. For both T-joint welding techniques, the same parameters were adopted: beam power Q = 2200 W and source velocity v = 3 m/min. In the case of one-sided welding, the angle of inclination of the beam relative to the connected elements was set $\alpha = 16^{o}$. Based on the numerical verification for single-beam welding assumed beam radius r = 0.35 mm, and s = 4 mm. In the case of the I-core joint type, r = 0.35 mm and penetration depth of the heat source h = 7 mm.

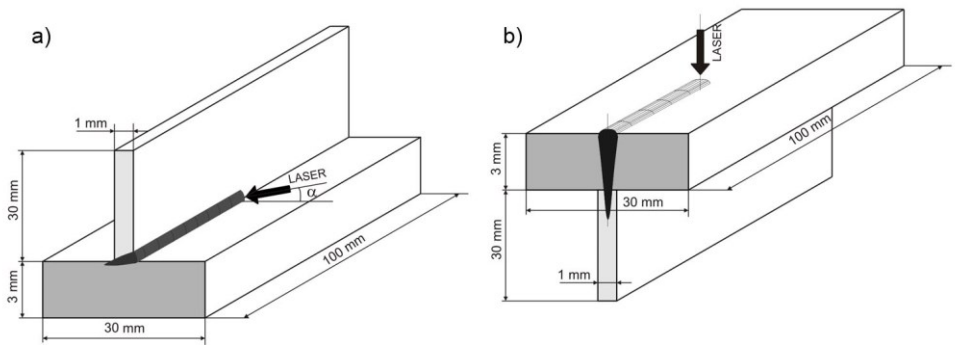

Fig. 2. Scheme of considered system: a) single side joint b) I-core

Both numerical models have the same MES mesh. The position of the heat source with respect to the coordinate system differs in both cases (Figure 3). In the case of single-sided welding, the origin of the coordinate system is on the contact edge of the joined elements. In the case of welding the I-core jont, the location of the coordinate system center is located on the upper surface, in the axis of symmetry of the model. In the contact planes between welded sheets was assumed perfect contact between the surfaces.

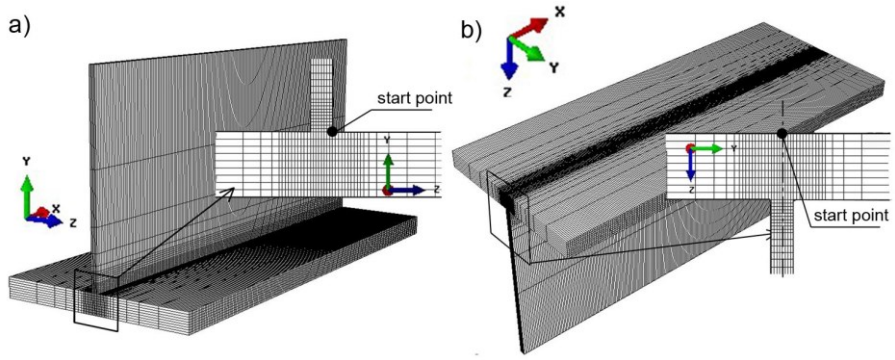

Fig. 3. Discretization of analyzed domain: a) single side joint, b) butt welded T-joint

Figure 3 presents numerical models with finite elements mesh. The highest density of the grid occurs at the welding line. In order to reduce the duration of the simulation at a further distance from the welding line, the mesh grid has a much larger dimension. Numerical calculations are performed separately. First, calculations of thermal phenomena and then mechanical calculations are performed. In the case of mechanical phenomena

analysis appropriate boundary conditions assumed in calculations are chosen to provide a static determination of considered system.

2.1 Thermal analysis

Energy conservation equation and Fourier's law are numerically solved in Abaqus FEA to determine temperature field in welded T-joints [4]. Equation in thermal analysis is completed by initial condition and boundary conditions of Dirichlet, Neumann and Newton type with heat loss due to convection, radiation and evaporation taken into considerations. The variational formulation of energy conservation equation is expressed as follows [13]:

$$\int_V \rho \frac{\partial U}{\partial t} \delta T \, dV + \int_V \frac{\partial \delta T}{\partial x_\alpha} \cdot \left(\lambda \frac{\partial T}{\partial x_\alpha} \right) dV = \int_V \delta T \, q_v \, dV + \int_S \delta T \, q_s \, dS \tag{1}$$

where λ is a thermal conductivity [W/m °C], $U = U(T)$ is a internal energy [J/kg], q_v is a laser beam heat source [W/m^3], $T = T(x_\alpha, t)$ is a temperature [°C], q_s is a boundary heat flux [W/m^2], δT is a variational function, ρ is a density [kg/m^3], $T = T(x_\alpha, t)$ is temperature [°C].

The numerical analysis of the welding process in Abaqus requires the implementation of an additional DFLUX numerical subroutine, written in the Fortran programming language. In the numerical subroutine, the power distribution of the heating source is modeled using the appropriate numerical models as well as its position relative to the joined elements and movement direction. Most widely used mathematical model of heat source power having Gaussian type distribution assumes a linear decrease of energy density along material penetration depth, expressed as follows [14]:

$$q_v(r,z) = \frac{Q}{\pi r_o^2 s} \exp\left[\left(1 - \frac{r^2}{r_o^2} \right) \right] \left(1 - \frac{z}{s} \right) \tag{3}$$

where Q is a laser beam power [W], r_0 is a beam radius [m], $r = \sqrt{x^2 + y^2}$ is actual radius [m], s is penetration depth [m], z is actual penetration [m].

In the case of one-sided laser beam welding, it is necessary to position the laser beam correctly in relation to the joined edges. In the additional numerical DFLUX subroutine, applying transformation formulas, the inclination of the welding beam is obtained by the assumed welding angle [5]. The scheme of the transformed system is shown in Figure 4.

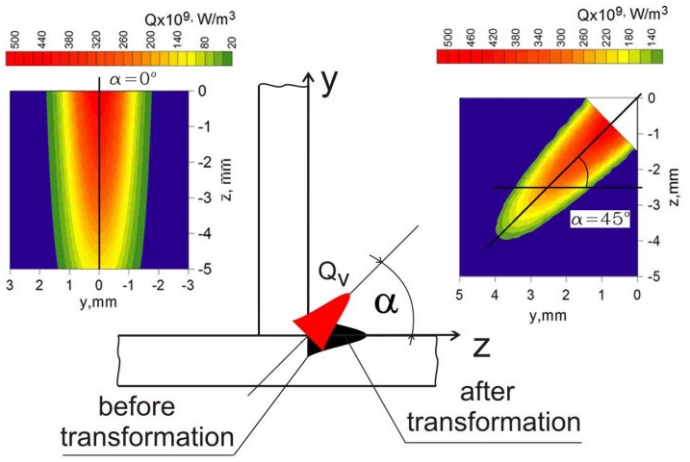

Fig. 4. Transformation of heat source power distribution [5]

2.2 Mechanical analysis

In the Abaqus program, the analysis of mechanical phenomena is based on the classical equation of equilibrium, which must be supplemented by initial conditions and boundary conditions. The analysis of phenomena is carried out in the elasto-plastic range [4, 15]:

$$\nabla \circ \dot{\boldsymbol{\sigma}}(x_\alpha, t) = 0, \qquad \dot{\boldsymbol{\sigma}} = \dot{\boldsymbol{\sigma}}^T \tag{4}$$

$$\dot{\boldsymbol{\sigma}} = \mathbf{D} \circ \dot{\boldsymbol{\varepsilon}}^e + \dot{\mathbf{D}} \circ \boldsymbol{\varepsilon}^e, \quad \boldsymbol{\varepsilon} = \boldsymbol{\varepsilon}^e + \boldsymbol{\varepsilon}^p + \boldsymbol{\varepsilon}^{Th} \tag{5}$$

$$\boldsymbol{\sigma}(x_\alpha, t_0) = \boldsymbol{\sigma}(x_\alpha, T_S) = 0, \ \boldsymbol{\varepsilon}(x_\alpha, t_0) = \boldsymbol{\varepsilon}(x_\alpha, T_S) = 0 \tag{6}$$

where: $\boldsymbol{\sigma}=\boldsymbol{\sigma}(\sigma_{ij})$ is stress tensor, x_α describes location of considered point (material particle), $(\circ)$ is inner exhaustive product, $\mathbf{D}=\mathbf{D}(T)$ is a tensor of temperature dependent material properties, $\boldsymbol{\varepsilon}$ is total strain, $\boldsymbol{\varepsilon}^e$ is elastic strain, $\boldsymbol{\varepsilon}^p$ is plastic strain and $\boldsymbol{\varepsilon}^{Th}$ is thermal strain.

The material model of 304 steel (X5CrNi18-10) has been included in the material module of Abaqus software. Thermo-mechanical properties varying on temperature are assumed in calculations for welded profiles made of adopted steel [4]. The figure shows the thermophysical and thermomechanical properties of 304 steel.

For material 304 stainless steel solidus temperature T_S = 1400°C, liquidus T_L = 1455°C, latent heat of fusion H_L=260×10^3 J/kg. Ambient temperature T_0 = 20°C and coefficient of heat exchange with the environment α_k = 100 W/m^2 °C.

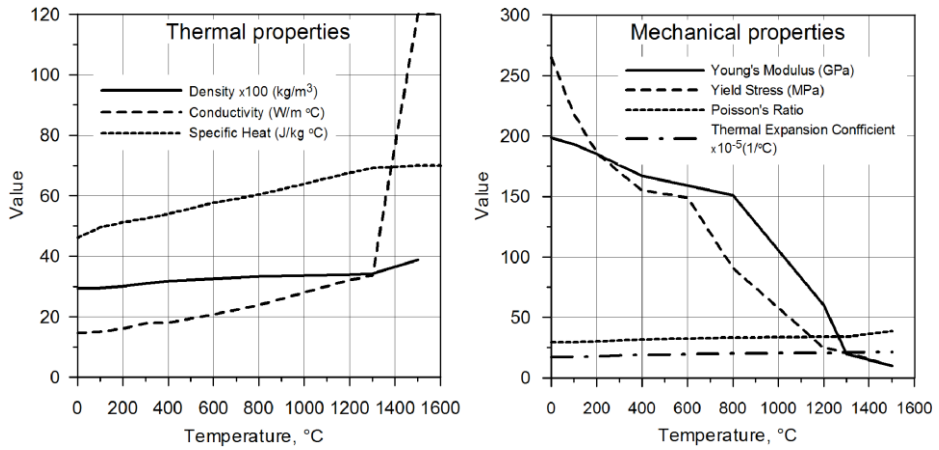

Fig. 5. Thermomechanical properties of X5CrNi18-10 stainless steel [4]

3 Results and discussion

Based on the developed numerical models for the assumed process parameters, simulation calculations are carried out. For both analyzed welding techniques, the temperature distributions and the shape and size of the melted zones are determined. In Figures 6 and 7, the boundaries of melted zones are marked with a solid line (isoline $T_L \approx 1455°C$). For single-sided welding based on the experimental studies in the literature [3] in order to determine the accuracy adopted numerical models compared the simulation results obtained (Figure 6b).

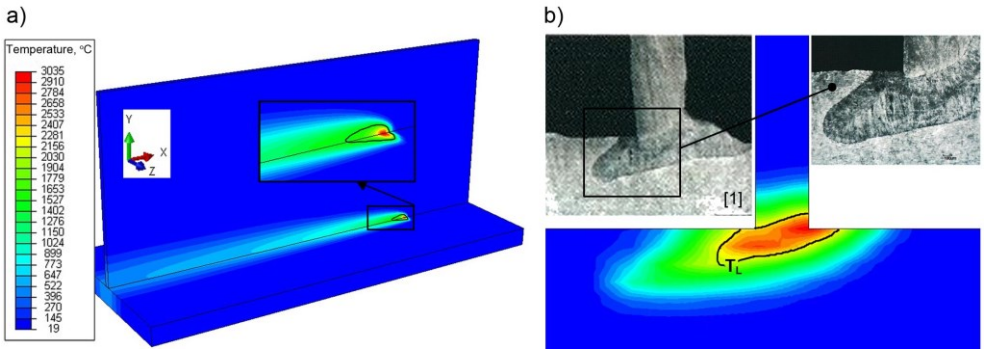

Fig. 6. Temperature distribution of the welded T-joint, a) comparing the numerically predicted shape of melted zone with the experiment b)

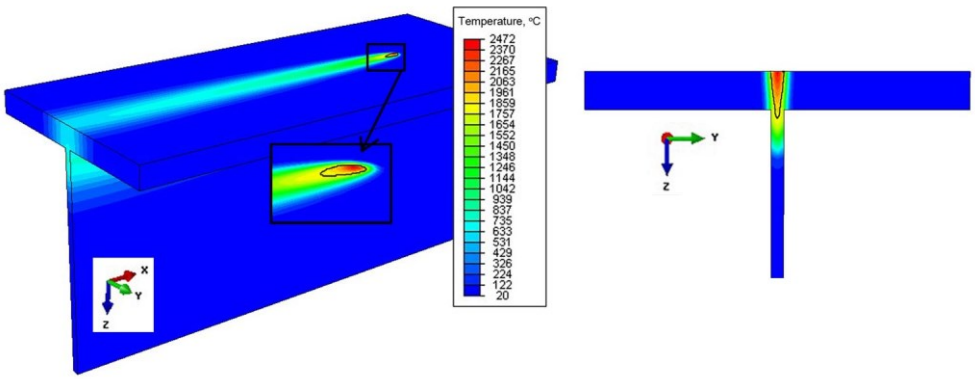

Fig. 7. Temperature distribution of the welded T-joint I-core type

Figure 8 presents the distributions of temproary residual stresses for two T-joint welded techniques. Numerical values of stresses obtained in both cases are similar. The maximum value of these stresses in both cases does not exceed 260 MPa. The concentration of stresses occurs in the welding line. In the case residual stresses, the maximum value does not exceed 225 MPa.

Figure 9 presents the numerically estimated displacement from half the length of welded joints. Significantly higher displacement values occur in the transverse direction to the welding line than in the longitudinal direction.

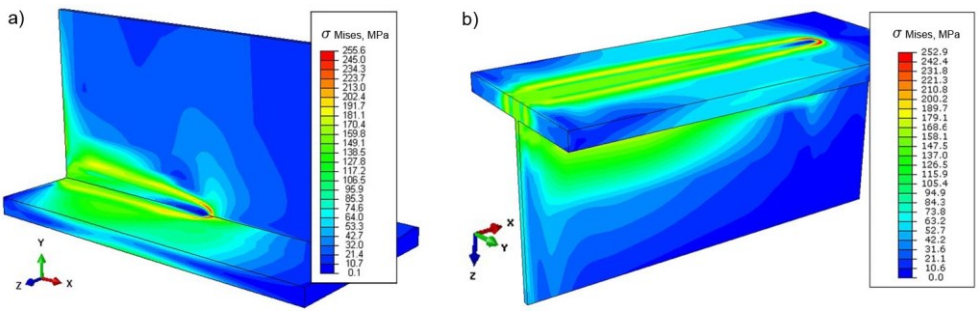

Fig. 8. Residual temporary reduced stress σ of welded T-joints a) one side welded T-joint, b) T-joint I-core type

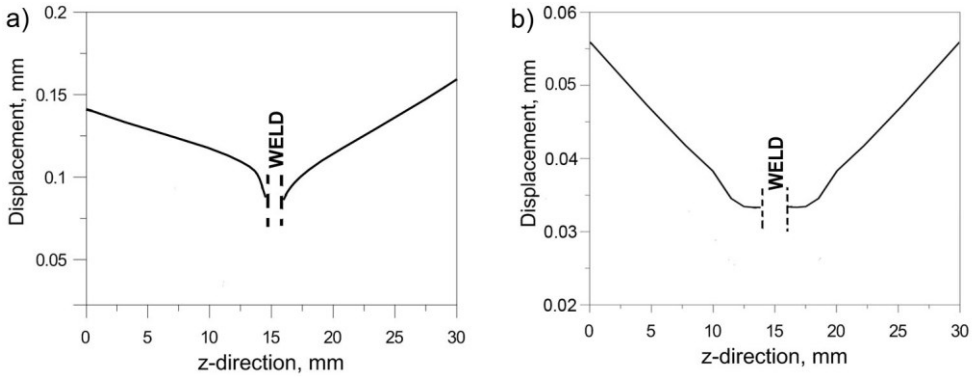

Fig. 9. Numerically estimated deflection U_y in cross section of welded T-joint; a) one side welded T-joint, b) T-joint I-core type

In the case of single-side welded T-joint, maximum displacement value occurs in the direction transverse to the welding line and does not exceed 0.17 mm. For the second welding technique to give a smaller displacement value, where the maximum value does not exceed 0.06 mm.

4 Conclusions

Numerical modeling of laser welding of T-joints using different welding techniques requires different process conditions that should be taken into account in calculations. In the case of numerical analysis of a single-sided welding, it is necessary to slope the heat source distribution at the appropriate welding angle. I-core type of T-joint require deep penetration of the material by the welding source in order to obtain a good penetration into the stiffening core.

In the analyzed T-joints, the greatest stresses occur in the welding line. The obtained stress values for both cases are comparable. The maximum value of reduced stresses does not exceed 225 MPa. Significant differences in values occur in the case of displacements. In both cases of welding T-joints, the largest displacements occur in the cross-section of the weld. For single-sided welding, the maximum value is 0.17 mm. However, in the case of I-core joint type 0.06 mm.

Developed numerical models can be a useful tool for pre-designing T-joint.

References

1. A.C. Oliveira, R.H.M. Siqueira, R. Riva, M.S.F. Lima, *One-sided laser beam welding of autogenous T-joints for 6013-T4 aluminium alloy.* Materials and Design, **65**, 726-736 (2015)
2. A. Unta, I. Poutiainen, A. Salminen, *Effects of sealing run welding with defocused laser beam on the quality of T-joint fillet weld.* Physics Procedia: 8th International Conference on Photonic Technologies LANE 2014. **56**, 497-506 (2014)
3. W. Piekarska, M. Kubiak, Z. Saternus, S. Stano, and T. Domański, *Numerical prediction of deformations in laser welded sheets made of X5Cr 18-10 steel.* Archives of Metallurgy and Materials, **60**, 3, 1965-1972 (2015)
4. S. Stano, J. Adamiec, J. Dworak, and M. Urbańczyk, *Badania procesu spawania laserowego złączy teowych z cienkich blach ze stali austenitycznej.* Biuletyn Instytutu Spawalnictwa, Poland, **5**, 141-151 (2016)
5. W. Piekarska, Z. Saternus, M. Kubiak and T. Domański, *Numerical analysis of the influence heat source slope on the shape and size of fusion zone in laser welded T-joint.* METAL 2016: 25th International Conference on Metallurgy and Material., Ostrava: TANGER, 688-693 (2016)
6. J. Kozak, *All steel sandwich panels – new possibilities introduced by laser welding techniques.* Przegląd Spawalnictwa, **10**, 53-59 (2007)
7. D. Deng, H. Murakawa, *FEM prediction of buckling distortion induced by welding in thin plate panel structures.* Comput Mater Sci, **43**, 591-607 (2008)
8. W. Piekarska, M. Kubiak, Z. Saternus, *Numerical simulation of deformations in T-joint welded by the laser beam.* Archiv Metall Mater., **58** (4) 1391-1396 (2013)

9. M. Kubiak, W. Piekarska, S. Stano, Z. Saternus, *Numerical Modelling Of Thermal And Structural Phenomena In Yb:Yag Laser Butt-Welded Steel Elements.* Arch Metall Mater, **60 (2)**, 821-828 (2015)
10. T. Domański, A. Sapietova, M. Saga, *Application Of Abaqus Software For The Modeling Of Surface Progressive Hardening*. Procedia Eng, **177**, 64-69 (2017)
11. M. Sapieta, A. Sapietova, V. Dekys, *Comparison of the thermoelastic phenomenon expressions in stainless steels during cyclic loading*. Metalurgija, **56** (1-2), 203-206 (2017)
12. M. Vasko, M. Blatnicky, P. Kopas, M. Saga, *Research of weld joint fatigue life of the AlMgSi07.F25 aluminium alloy under bending-torsion cyclic loading*. Metalurgija, **56** (1-2), 94-98 (2017)
13. SIMULIA, *Abaqus FEA theory manual*. Version 6.7, Dassault System (2007)
14. S.A. Tsirkas, P. Papanikos, Th. Kermanidis, *Numerical simulation of the laser welding process in butt-joint specimens*. J Mater Process Tech, **134**, 59-69 (2003)
15. A. Bokota, T. Domański, M*odelling and numerical analysis of hardening phenomena of tools steel elements*. Archives Of Metallurgy And Materials, 575-587 (2009)